

Indian Journal of Chemistry  
Vol. 58A, November 2019, pp. 1187-1193

## A novel FRET probe for determination of fluorescein sodium in aqueous solution: Analytical application for ophthalmic sample

Dhanshri V Patil<sup>a,\*</sup> & Vishal S Patil<sup>b</sup>

<sup>a</sup>Department of Chemistry, Krishna Mahavidyalaya, Rethare Bk 415 108, Maharashtra, India

<sup>b</sup>Department of Chemistry, Sanjeevan Engineering & Technology Institute, Panhala 416 201, Maharashtra, India

Email: [ntp.phy@gmail.com](mailto:ntp.phy@gmail.com)

Received 7 March 2019; revised and accepted 15 October 2019

Fluorescent pyrene nanoparticles (PyNPs) have been prepared by a reprecipitation method in the presence of sodium dodecyl sulphate (SDS) as a stabilizer. The formation of PyNPs has been confirmed by dynamic light scattering (DLS), UV-visible absorption spectroscopy, fluorescence spectroscopy and excited state lifetime measurements. DLS results of PyNPs shows a narrow size distribution with average particle size of 77.4 nm and negative zeta potential. The systematic FRET experiments performed by measuring fluorescence quenching of PyNPs with successive addition of FL-Na analyte exploited the use of PyNPs as nanoprobe for detection of FL-Na in aqueous solution. The fluorescence of PyNPs has been quenched by FL-Na and quenching has been in accordance with the Stern-Volmer relation. The distance  $r$  between the donor (PyNPs) and acceptor (FL-Na) molecules has been obtained according to the fluorescence resonance energy transfer. The fluorescence quenching results have been used further to develop an analytical method for estimation of fluorescein sodium from ophthalmic samples available commercially in the market.

**Keywords:** Fluorescent pyrene nanoparticles, Fluorescein sodium, Fluorescence resonance energy transfer

Fluorescein sodium (FL-Na), also called uranine, is a non-toxic, low molecular weight and highly water-soluble dye, shows the physical property of fluorescence and commonly used as a quantitative fluorophore for studying different tissues of the eye<sup>1-3</sup>. FL-Na shown in Fig. 1 is extensively used as a diagnostic tool in the field of ophthalmology and optometry. It is available as sterile single use sachets containing lint-free paper applicators soaked in FL-Na<sup>4</sup>. It has a  $pK_a$  of 6.4 and its ionization equilibrium leads to pH-dependent absorption and emission over the range of 5 to 9. It can exist in seven prototropic forms, each of which possesses its own distinct spectral properties<sup>5</sup>. In neutral solutions, such as water and methanol (which also act as polar solvents) it exists mainly as dianion. It is widely used as fluorophore in the biosciences and as a fluorescent tracer for many applications<sup>6</sup>. Few methods have been used for detection and estimation of dyes<sup>7-9</sup>. A direct fluorimetric method requires separating the analyte from interfering constituents in the samples and having absorption in the region of analyte molecule. By contrast the fluorescence quenching/enhancement methods have high sensitivity and more simple detection and do not need separation of analyte

molecules from other interfering constituents<sup>10-13</sup>. Therefore, the development of sensitive and selective sensors for FL-Na is of current interest.

Fluorescent organic nanoparticles (FONs) of low molecular weight functional compounds found special interest because of high variability and flexibility in materials and method of nanoparticles preparation<sup>14-15</sup>. Organic nanoparticles (ONs) occupy the intermediate state between isolated molecules and the bulk crystal. It is observed that most of the fluorescent organic materials belonging to the class of polynuclear aromatic hydrocarbons (PAHs) are water insoluble and gives their monomer emission in lower wavelength regions. PAHs are used as a fluorescent probe for the fluorescence quenching process<sup>16-18</sup>. Among the PAHs, Perylene and Pyrene are popular because of their large lateral  $\pi$ -orbital stacking between molecules and are most widely used probes

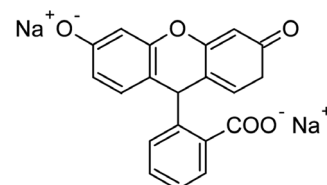


Fig. 1 — Structure of fluorescein sodium.

for fluorimetric detection in an aqueous micellar medium<sup>19</sup>. Therefore, these materials are often used as fluorescent bio-probes, sensors and organic electronic devices. Thus, to put this monomer emission in long wavelength region, our strategy is to synthesize the water soluble core shell pyrene nanoparticles (PyNPs) giving their nanomer (dimer) emission in higher wavelength region. The technique of analysis is based on FRET from pyrene nanoprobe to analyte molecule. A simple, selective and sensitive fluorimetric method is developed for estimation of FL-Na from ophthalmic samples.

## Materials and Methods

### Reagents and instruments

Pyrene (Merck-Schuchart) and fluorescein-sodium (Hi-media) were used after purity testing. The purity of the compounds was checked by recording their fluorescence spectra at different excitation wavelengths and comparing the values obtained with those reported in the literature. SDS was from S-D Fine Chemicals Ltd., and used to generate micellar medium by dissolving in ultrapure water (Millipore, France).

The average particle size was measured by using Dynamic Light Scattering (DLS) on Particle Sizing Systems, Inc. Santa Barbara, Calif., USA. The life time was measured on Time-Correlated Single-Photon Counting (TCSPC) (Horiba Time Resolve Spectro fluorimeter). The Scanning Electron Micrograph (SEM) was recorded on Scanning Electron Microscope (JEON-6360, Japan) to examine the morphology and size of nanoparticles. The fluorescence and fluorescence excitation measurements were carried out on a PC-based spectrofluorimeter JASCO, Japan (Model FP-750). The absorption spectra were recorded on a UV-VIS-NIR spectrophotometer [Shimadzu UV-3600].

### Preparation of PyNPs by reprecipitation method and general procedure

The reprecipitation method has been developed in our laboratory and applied successfully to obtain the PyNPs. The method involved preparation of dilute solution of pyrene ( $6.82 \times 10^{-3}$  mol L<sup>-1</sup>) in acetone which yielded the monomer fluorescence when recorded under the appropriate excitation wavelength. The PyNPs prepared without surfactant was found to be less photo stable and therefore not suitable for FRET studies. The photo stability of the nanoparticles was studied by recording fluorescence spectra after a certain interval of time. The photo degradation of

PyNPs stabilized by surfactant is seen to be very slow, hence found suitable for FRET studies. The sodium dodecyl sulphate [SDS] surfactant was used and it is found that the SDS solution below critical micelle concentration yielded PyNPs with narrow size distribution, dispersity and with high photo stability. Therefore,  $3.6 \times 10^{-3}$  mol L<sup>-1</sup> SDS concentration was selected for synthesis of PyNPs. The solution of pyrene in acetone was filled in micro syringe and then purged into aqueous solution of SDS under vigorous stirring. The stirring was carried out for about one hour and further subjected to ultrasonication for about 30 min so as to prolong the stability.

The stock solution of FI-Na ( $1 \times 10^{-4}$  mol L<sup>-1</sup>) was prepared by dissolving calculated amount directly in water, then further diluted to  $5 \times 10^{-5}$  mol L<sup>-1</sup> by the same solvent and the as prepared PyNPs solution was used to carry out the experiment. In a 10 mL comparison tube 2.5 mL of PyNPs ( $1.4 \times 10^{-4}$  mol L<sup>-1</sup>) solution was added. The quantity of PyNPs was kept constant while that of FI-Na was varied from 0.0 to 2.4 mL and diluted to 5 mL by using water. The quartz cuvettes were used for absorption; excitation and emission measurements and slit widths were fixed at 5 nm during excitation and emission measurements.

### Characterization of PyNPs

#### Particle size analysis

The particle size histogram of PyNPs prepared by using SDS is shown in Fig. 2. The strong  $\pi$ - $\pi$  stacking interactions between adjacent molecules would facilitate the stacking of molecules onto one another<sup>20,21</sup>. The aggregates of pyrene are stabilized by using SDS surfactant solution. It is known that the surfactant prevents the agglomeration of the aggregates by encapsulation and removes nanoparticles from solution which results in stable colloidal dispersion<sup>22</sup>.

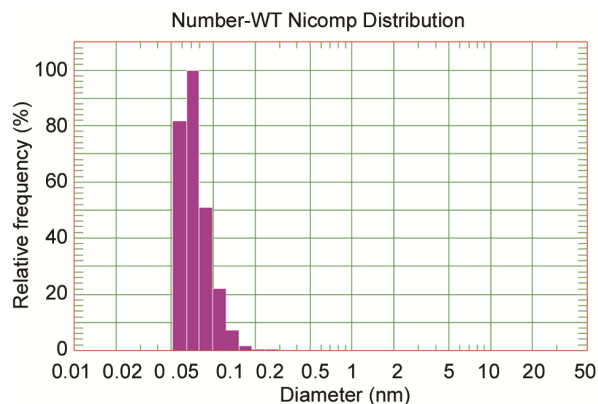


Fig. 2 — Representative particle size distribution histogram of PyNPs.

### Excited state life time of nanoparticles

The time resolved fluorescence spectra of pyrene in acetone and PyNPs is shown in Fig. 3. The formation of nanoparticles results into change in life time of electronically excited state, when compared with life time of sample molecule in solution. The fluorescence life time are obtained from the fluorescence decay profile recorded at constant excitation and emission wavelength of the sample solution and nanoparticles suspension. It is seen that the life time of the excited state of the PyNPs (6.6 ns) is longer than that of corresponding pyrene solution (1.43 ns) in acetone. It is known that aggregation and molecular interactions tend to prolong the life time. Also, the complex state of organic molecule generally exhibits a longer decay time as compared to that of the initially excited state<sup>23</sup>. Relatively longer life time of PyNPs (6.6 ns) than its pyrene solution (1.43 ns) proves that the pyrene monomers aggregates by self assembly to form nanostructures. The long lifetimes of PyNPs compared with that of monomer solution can be easily understood from the fact that the formation of aggregated nanoparticles restricts the molecular rotation and vibration of molecules and thus enhances the emission lifetime of PyNPs<sup>8</sup>. Hence the change in life time is supportive information for confirmation of nanoparticles formation.

### Scanning Electron Microscopy (SEM)

SEM photomicrograph of air dried layer of PyNPs capped with SDS surfactant is presented in Fig. 4. It reveals distinct spheres, clearly indicating that the aggregated particles are spherical and relatively mono dispersed in shape. The average particle size estimated from SEM images is 95 nm and seen to be significantly greater than the size obtained from DLS results (77.4 nm) because of the agglomeration of the

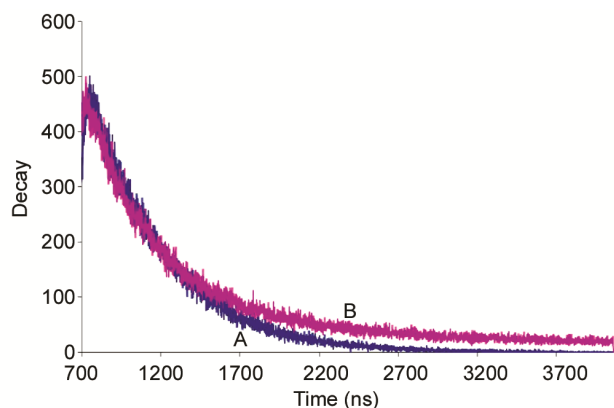


Fig. 3 — Time resolved fluorescence spectra of pyrene in acetone (A) and pyrene nanoparticles (B).

nanoparticles during drying of suspension on glass substrate in an attempt made to obtain thin film of PyNPs.

### Absorption spectroscopy

The absorption spectrum of dilute solution of pyrene in ethanol (A) and PyNPs (B) is shown in Fig. 5. The absorption spectrum of pyrene in ethanol is structured with overlap of three absorption bands in the region 300–350 nm. On the contrary, absorption band of PyNPs is red shifted from the spectrum of dilute solution of pyrene in ethanol and gets broadened. The red shift is because of strong  $\pi$ - $\pi$  stacking of the neighboring molecules in the nanoparticles aggregation. The planar pyrene molecules in SDS stabilised by self-assembled nanoclusters are held together by intermolecular  $\pi$ - $\pi$  stacking (J-aggregates) confirmed by a bathochromic shift in UV-visible absorption spectrum of pyrene nanoparticles<sup>8</sup>.

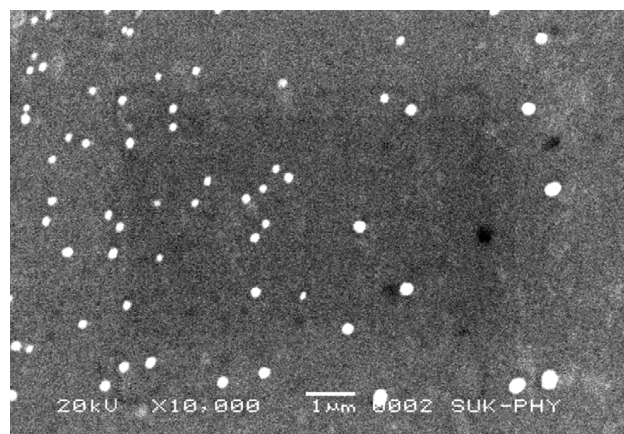


Fig. 4 — SEM photomicrograph of air dried layer of PyNPs capped with SDS surfactant.

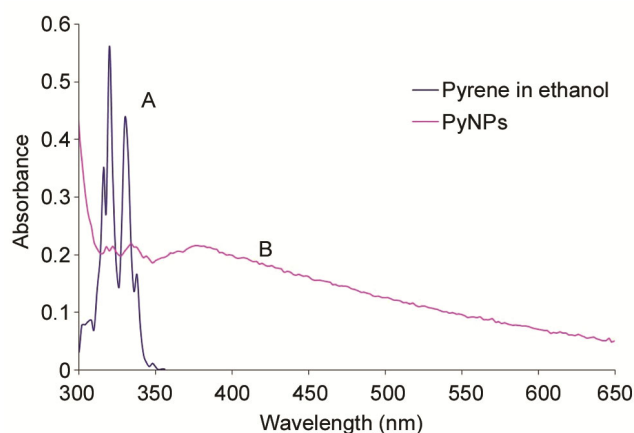


Fig. 5 — Absorption spectra of pyrene in ethanol dilute solution (spectrum- A) and PyNPs (spectrum- B).

### Excitation and fluorescence spectroscopy

Excitation and fluorescence spectra of dilute solution of pyrene in acetone and prepared PyNPs are shown in Fig. 6 and Fig. 7 respectively. The excitation spectrum of the pyrene in acetone dilute solution (A) is shown in Fig. 6 is also structured and spectral features are identical with the absorption spectrum (spectrum- A in Fig. 5). However, the excitation spectrum of the PyNPs (B) shows three bands in the region 275–390 nm. The lack of vibrational fine structure suggests aggregation of pyrene molecules to form nanoparticles in the surfactant solution. The fluorescence spectrum of PyNPs (spectrum- B, Fig. 7) monitored at excitation wavelength 360 nm is a structureless broad band with maximum emission at 466 nm. The monomer emission band is not seen in the spectrum of PyNPs suspension.

Though, the emission is observed only due to the excitation of aggregated molecules, this band cannot be

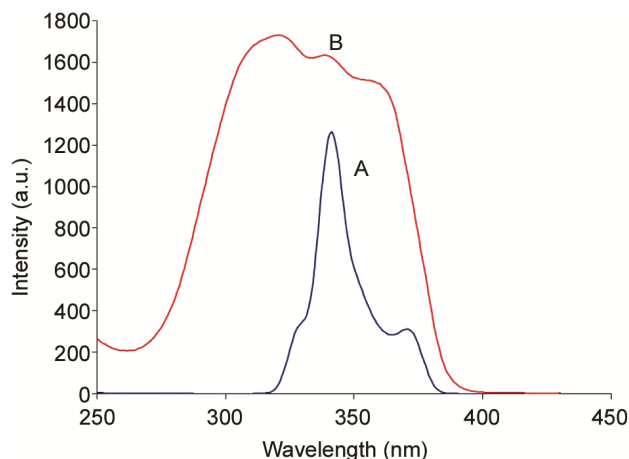


Fig. 6 — Excitation spectra of (A) dilute solution of pyrene in acetone and (B) PyNPs.

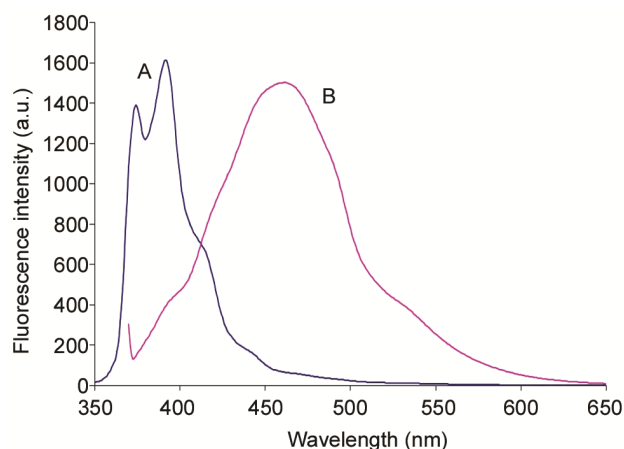


Fig. 7 — Fluorescence spectra of the dilute solution of pyrene in acetone (spectrum- A) and PyNPs in suspension (spectrum-B).

confused with excimer emission of pyrene shown to occur at 471 nm due to excimer species formed between excited and ground state pyrene molecule by lateral  $\pi$ -orbital overlapping<sup>20</sup>. Hence, the aggregated pyrene is dimer in nanoparticle. The aggregated PyNPs absorbs UV-photon of wavelength 360 nm corresponding to its excitation energy and an excited aggregate deactivates radiatively to give excimer like emission.

The photophysical studies led us to select PyNPs as probe (donor) and FI-Na as energy acceptor. These interactions have resulted in quenching of fluorescence of PyNPs and established the analytical relation for determination of FI-Na from pharmaceutical sample. The fluorescence spectrum of PyNPs (spectrum-D) exhibits significant spectral overlap with excitation spectrum of FI-Na (spectrum-A) is shown in Fig. 8. This indicates that the excited PyNPs molecule can transfer its excitation energy to FI-Na which is in the ground state.

## Results and discussion

### UV-visible absorption and fluorescence spectroscopy

#### UV-visible absorption study

The UV-visible absorption spectra of PyNPs in absence and presence of varying concentrations of FI-Na are shown in Fig. 9. The absorption spectrum of PyNPs (spectrum-1) shows two bands one at 265 nm due to aromaticity and another broad band peaking at 377 nm in the region 320–500 nm due to strong  $\pi - \pi$  stacking interactions of the neighboring molecules in the nanoparticles aggregation<sup>20</sup>. By contrast the spectrum of FI-Na without PyNPs (spectrum-10) shows two bands one at 236 nm due to  $\pi \rightarrow \pi^*$  transition and another pronounced  $n \rightarrow \pi^*$  band at 489 nm<sup>24</sup>. Furthermore, with increasing concentrations of FL-Na,

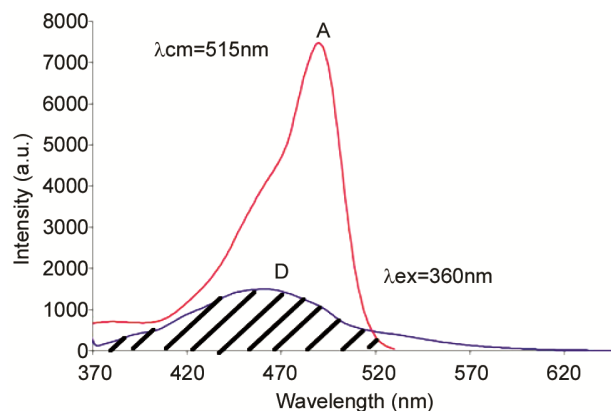


Fig. 8 — Spectral overlap between emission of PyNPs (D) and excitation of FI-Na (A).



the absorption intensity of PyNPs peak at 377 nm increases slightly without any spectral shift. Also, the absorption bands of FI-Na at 489 nm increases with increase in its concentration. These results showed the absence of ground state interactions between PyNPs and FI-Na and confirm dynamic quenching process in the present system.

#### Fluorescence quenching of PyNPs by FI-Na

The fluorescence spectra of PyNPs recorded in absence and presence of different concentrations of FI-Na are shown in Fig. 10, in the range 370–650 nm. When a fixed concentration of PyNPs was titrated with different amounts of FI-Na, a remarkable decrease in fluorescence intensity of PyNPs was observed. In addition, a blue spectral shift at the maximum wavelength of PyNPs fluorescence

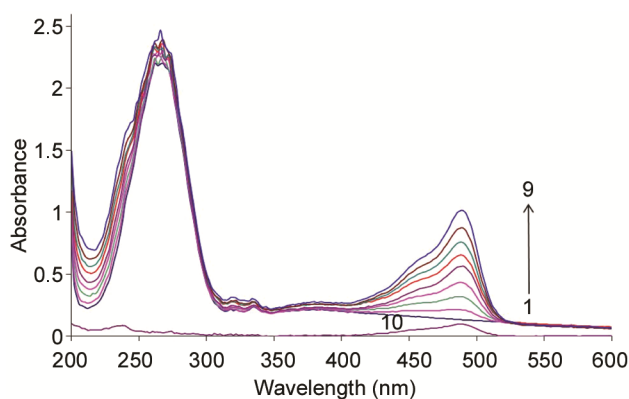


Fig. 9 — UV-visible absorption spectra of PyNPs ( $6.8 \times 10^{-5} \text{ mol L}^{-1}$ ) in absence and presence of different concentrations of FI-Na (spectra from 1 to 9) corresponding to  $[0.0, 0.3, 0.6, 0.9, 1.2, 1.5, 1.8, 2.1, 2.4] \times 10^{-5} \text{ mol L}^{-1}$  and spectrum-10 is of pure FI-Na at 305 K.

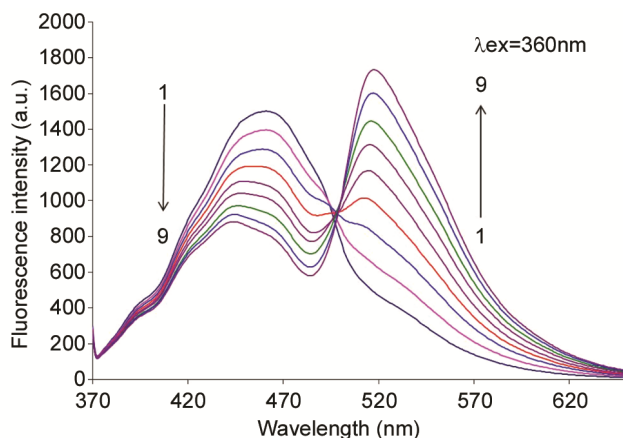


Fig. 10 — Fluorescence quenching spectra of PyNPs-FI-Na system, from 1 to 9:  $[\text{PyNPs}] = 6.8 \times 10^{-5} \text{ mol L}^{-1}$ ;  $[\text{FI-Na}] = (0.0, 0.3, 0.6, 0.9, 1.2, 1.5, 1.8, 2.1, 2.4) \times 10^{-5} \text{ mol L}^{-1}$  at 305 K.

emission is seen from 461 nm to 443 nm, when the solution of FI-Na was added successively. This suggests that the addition of FI-Na changes the polarity of the hydrophobic microenvironment around PyNPs and resulting in the destabilization of PyNPs<sup>25</sup>.

#### Stern-Volmer plot and energy transfer between PyNPs and FI-Na

The Stern-Volmer (S-V) plot of  $F_0/F$  versus  $[\text{FI-Na}]$  is shown in Fig. 11. It is evident from figure that the S-V plot is linear in the concentration range of acceptor studied. The linearity of this plot indicates only one type of quenching occurred in present PyNPs-FI-Na system<sup>26</sup>. The fluorescence quenching data is analyzed by using well known S-V equation:

$$\frac{F_0}{F} = 1 + k_q \tau_0 [Q] = 1 + K_{sv} [Q] \quad \dots (1)$$

Where  $F_0$  and  $F$  are the fluorescence intensities in the absence and presence of quencher FI-Na respectively,  $k_q$  is the quenching rate constant and  $\tau_0$  is the average lifetime of the PyNPs in absence of quencher ( $\tau_0 = 6.5 \times 10^{-9} \text{ s}$ )<sup>8</sup>,  $K_{sv}$  is the S-V quenching constant,  $[Q]$  is the concentration of quencher, FI-Na. From the slope of the plot, value of  $K_{sv}$  obtained is  $2.974 \times 10^4 \text{ L mol}^{-1}$ .

$$k_q = K_{sv} / \tau_0 \quad \dots (2)$$

Also, from the Eqn 2, value of  $k_q$  obtained  $4.506 \times 10^{12} \text{ L mol}^{-1} \text{ s}^{-1}$ .

The energy transfer is related not only to the distance between the donor and the acceptor ( $r$ ), but also to the critical energy transfer distance ( $R_0$ ). The distance between the donor (PyNPs) and the acceptor (FI-Na) can be calculated by using the Förster's

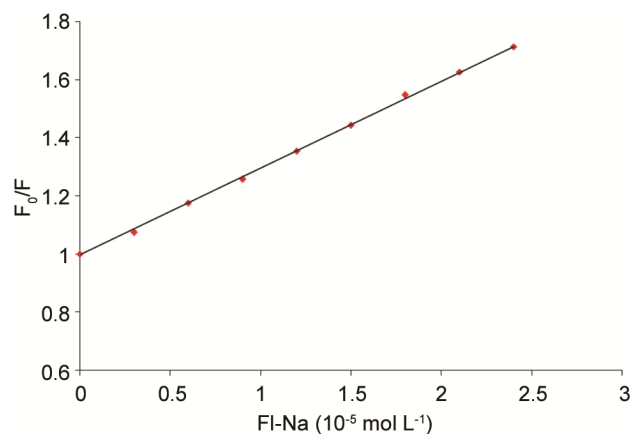


Fig. 11 — Stern-Volmer plot of  $F_0/F$  vs FI-N ( $10^{-5} \text{ mol L}^{-1}$ ).

non-radiative energy transfer theory. The efficiency of energy transfer ( $E$ ) is also an important aspect.

$$E = \left(1 - \frac{F}{F_0}\right) = \frac{R_0^6}{R_0^6 + r^6} \quad \dots (3)$$

$$R_0^6 = 8.79 \times 10^{-25} K^2 N^{-4} \phi J \quad \dots (4)$$

Where  $R_0$  is the critical distance at which the transfer efficiency equals to 50%.  $K^2$  is the spatial orientation factor for the donor and acceptor dipoles and  $K^2$  is usually assumed to be equal<sup>27</sup> to 0.667, which is appropriate for dynamic random averaging of the donor and acceptor positions,  $N = 1.336$  (the refractive index of medium)<sup>8</sup> and  $\phi = 0.4765$  the fluorescence quantum yield of donor PyNPs in the absence of the acceptor FL-Na<sup>8</sup>.

$$J = \int \frac{f(\nu)E(\nu)d\nu}{\nu^4} \quad \dots (5)$$

$J$  expresses the degree of spectral overlap between the donor emission and the acceptor excitation as shown in Figure 8. Hence, by using equations 3 to 5, the parameters calculated are,  $J = 0.57 \times 10^{-13} \text{ cm}^3 \text{ L mol}^{-1}$ ,  $R_0 = 41.38 \text{ Å}$ ,  $E = 0.2676$ , and  $r = 4.89 \text{ nm}$ ,  $r < 7 \text{ nm}$ . These data suggests that the energy transfer from PyNPs to FI-Na can occur with high probability<sup>28</sup>.

#### Analysis of FI-Na from pharmaceutical formulations

The fluorescein sodium is available in the form of ophthalmic strip by the name Fluoro Touch. Therefore, the proposed quenching method was applied for estimation of fluorescein sodium. Fluoro Touch strip is used for the detection of damage in corneal surface, evaluating ocular adaptability to hard contact lens and inspecting leakage from incision caused by ophthalmic surgery. Thus, for analysis purpose, strip was dissolved in water and diluted to the required volume. Then, this solution was used for the quenching experiment along with the standard set given in experimental section. The calibration plot for the determination of FI-Na was constructed by plotting  $F_0/F$  versus FI-Na concentration as shown in Fig. 12. The plot depicts a good linear relationship between the fluorescence quenching intensity and concentration of FI-Na, with a correlation coefficient ( $R$ ) of 0.998. The corresponding linear regression equation is  $y = 0.279x + 1$  and were used to calculate unknown concentrations of FI-Na from pharmaceutical dissolutions. The Relative Standard Deviation (RSD) is 1.02 %. The results obtained are in

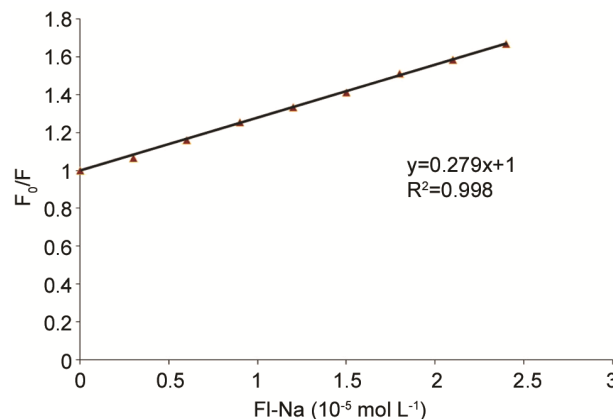


Fig. 12 — Calibration graph for analysis of FI-Na.

Table 1 — Determination of fluorescein sodium in ophthalmic strip

Sample	Composition	Amount of fluorescein sodium		S.D.	R.S.D. (%)
		Certified	Found*		
Fluoro Touch (Fluorescein sodium ophthalmic strip U. S. P.)	Fluorescein sodium I.P. 1 mg	1 mg	0.983 mg	0.01	1.02

\*Average of three determinations.

good agreement with certified values given in Table 1. The limit of detection (LOD) of the method was  $5.0582 \times 10^{-5} \text{ mol L}^{-1}$ , calculated by the equation  $\text{LOD} = (3\sigma/k)$ , where  $\sigma$  is the standard deviation of the y-intercept of the regression lines and  $k$  is the slope of the calibration graph<sup>9</sup>. Thus, the proposed method is very simple, selective and reproducible for analysis of pharmaceutical samples containing FI-Na.

#### Conclusions

The molecular interactions between PyNPs and FI-Na were investigated by measuring quenching of fluorescence and UV-visible absorption. The fluorescence quenching of PyNPs on successive addition of FI-Na with blue spectral shift results in destabilization of PyNPs. Also, the fluorescence of PyNPs was quenched by FI-Na and proved the validity of Stern-Volmer (S-V) relation. The distance ( $r$ ) between PyNPs and FI-Na was estimated to be 4.89 nm. The quenching data is successfully applied to estimate quantitatively FI-Na from pharmaceutical sample available as fluoro touch in the market. Thus, the method developed is simple, selective and reproducible.

#### Acknowledgement

The authors gratefully acknowledge Department of Science and Technology (DST) and University Grants

Commission (UGC), New Delhi, for providing Grants to the Department of Chemistry, Shivaji University, Kolhapur, under FIST and SAP program, respectively. One of the author (D. V. Patil) thanks to UGC, for the award of UGC-SAP Junior Research fellowship.

## References

- 1 Ibrahem M D & Mesalhy S, *J Advanc Res*, 1 (2010) 361.
- 2 Fineschi V, Monasterolo G, Rosi R & Turillazzi E, *J Forensic Sci Int*, 100 (1999) 137.
- 3 Mota M C, Carvalho P, Ramalho J & Leite E, *Int Ophthal*, 15 (1991) 321.
- 4 Hughes F N, *Can Med Asso J*, 80 (1959) 997.
- 5 Lavis L D, Rutkoski T J & Raines R T, *Anal Chem*, 79 (2007) 6775.
- 6 Song A, Zhang J, Zhang M & Shen T, *Colloids Surf A*, 167 (2000) 253.
- 7 Chiang T L, Wang Y C & Ding W H, *J Chin Chem Soc*, 59 (2011) 1.
- 8 Bhopate D P, Mahajan P G, Garadkar K M, Kolekar G B & Patil S R, *RSC Adv*, 4 (2014) 63866.
- 9 Bhopate D P, Mahajan P G, Garadkar K M, Kolekar G B & Patil S R, *Luminescence*, 30 (2015) 1055.
- 10 Patil D T, Bhattar S L, Kolekar G B & Patil S R, *J Solution Chem*, 40 (2011) 211.
- 11 Patil D T, Mokashi V V, Kolekar G B & Patil S R, *Luminescence*, 28 (2013) 821.
- 12 Patil D V, Patil V S, Sankpal S A, Kolekar G B & Patil S R, *J Incl Phenom Macrocycl Chem*, 90 (2018) 99.
- 13 Dang Y Q, Ren S Z, Cai J, Liu G, Zhang Y & Qui J, *Indian J Chem Sec A*, 57 A (2018) 1270.
- 14 Lei Z, Zhongxing L, Xiaoran L, Shengbiao L, Jun X, Bo P & Wei H, *Chem Phys Lett*, 420 (2006) 480.
- 15 Krishna P, Ravi A & Thomas K, *J Photochem Photobiol A: Chem*, 215 (2010) 179.
- 16 Patil S R, Mote U S, Patil S R, Lee S H & Kolekar G B, *J Rare Earths*, 28 (2010) 329.
- 17 Mote U S, Patil S R & Kolekar G B, *J Mol Liq*, 157 (2010) 102.
- 18 Bhattar S L, Kolekar G B & Patil S R, *J Lumin*, 130 (2010) 355.
- 19 Bhopate D P, Kolekar G B, Garadkar K M & Patil S R, *Anal Methods*, 5 (2013) 5324.
- 20 Zhang X, Zhang X, Shi W, Meng X, Lee C & Lee S, *J Phys Chem B*, 109 (2005) 18777.
- 21 Yan H & Li H, *Sens Actuator B*, 148 (2010) 81.
- 22 Gong X, Milic T, Xu C, Batteas J D & Drain C M, *J Am Chem Soc*, 124 (2002) 14290.
- 23 Fox M A & Chanon M, *Photoinduced Electron Transfer Part A*, Elsevier, New York (1988).
- 24 Skoog D A, Holler F J & Nieman T A: *Principles of Instrumental Analysis*; 5<sup>th</sup> Ed., Saunders Sunburst Series (1998).
- 25 Yuan T, Weljie A M & Vogel H, *J Biochem*, 37 (1998) 3187.
- 26 Das P, Mallick A, Purkayastha P, Halder B & Chattopadhyay N, *J Mol liq*, 130 (2007) 48.
- 27 Cao S, Wang D, Tan X & Chen J, *J Solution Chem*, 38 (2009) 1193.
- 28 Hu Y J, Lu Y, Shen X S, Fang X Y & Qu S S, *J Mol Struct*, 738 (2005) 143.